POLITECNICO DI TORINO
Repository ISTITUZIONALE

Solving the More Difficult Aspects of Electric Motor Thermal Analysis in Small and Medium Size Industrial Induction Motors

(Article begins on next page)

19 April 2024

Solving the More Difficult Aspects of Electric Motor Thermal Analysis in Small and Medium Size Industrial Induction Motors

Dave Staton, Aldo Boglietti, and Andrea Cavagnino

Abstract—With the ever-increasing pressure on electric motor manufacturers to develop smaller and more efficient electric motors, there is a need for more thermal analysis in parallel with the traditional electromagnetic design. Attention to the thermal design can be rewarded by major improvements in the overall performance. Technical papers published to date highlight a number of thermal design issues that are difficult to analyze. This paper reviews some of these issues and gives advice on how to deal with them when developing algorithms for inclusion in design software.

Index Terms—Induction motors, thermal analysis, thermal models.

I. INTRODUCTION

MOTOR performance is governed by electromagnetic (EM) and thermal design. Both designs are, in fact, interrelated. Not only are the losses dependent on the temperatures and vice-versa, but more complex issues arise at the design stage. Examples of such complexities are the fact that it is usually easier to dissipate stator iron loss than copper loss due to its closer proximity to the housing (the optimum balance between copper and iron loss should therefore be examined at the design stage for the required torque/speed profile); lower loss lamination materials have reduced thermal conductivities; the end-winding losses have local air cooling (or conductive cooling if potted), etc. Given this interrelation, it is surprising that the thermal design usually receives less attention that the EM design. This is especially true in small- and medium-sized motors.

Recently, attention to the thermal design has been rewarded by major improvements in the overall performance. Raised awareness of the importance of thermal issues has led to increased work devoted to the development of electric motor thermal models. However, the number of published papers relating to the thermal analysis of electric motors is still much less than those associated with EM analysis. The published papers to date highlight a number of thermal design issues that are more difficult to analyze than others. This paper reviews a number of difficult design aspects and gives advice on how to deal with them when developing design algorithms suitable for inclusion in thermal lumped circuit models.

Fig. 1. TEFC motors used to generate test data.

Test data are presented to illustrate the difficulties, help develop design algorithms, and provide default data. Fig. 1 shows examples of some of the total enclosed fan-cooled (TEFC) motors tested to generate data for this work. All of the motors are thermally monitored with PT100 sensors. Three sensors are on the end winding (one for each phase) and another sensor is inserted inside a stator slot. The last sensor is in a hole positioned in the stator core. This allows measurement of the winding and iron core temperatures during the tests. The housing temperature can be measured by means of a digital thermometer taking into account several positions on the housing surface.

The problems examined in this paper are:

- interference gaps between components;
- winding models suitable for identifying hot-spots and accounting for nonperfect impregnation;
- convection cooling from the surface of the machine including problems of open axial channel fin leakage and blockage (due to lugs and terminal boxes);
- turbulent cooling around the end-winding and axial end sections of the machine (including fanning effects of induction motor wafters and synchronous/switched-reluctance motor salient poles);
- heat transfer across the air gap including complexities such as slot openings and salient poles;
- uncertainty of material property data;
- bearing and end-shield models.

Most of the theory shown in this paper is included in a thermal analysis package for electrical machines.

D. Staton is with Motor Design Ltd., Shropshire SY12 9DA, U.K. (e-mail: dave.staton@motor-design.com).

A. Boglietti and A. Cavagnino are with the Dipartimento di Ingegneria Elettrica Industriale, Torino 10129, Italy (e-mail: aldo.boglietti@polito.it; andrea.cavagnino@polito.it).

TABLE I
CONTACT RESISTANCE AND INTERFACE GAP FROM HOLMAN [1]

	RMS Roughness [mm]	Contact Resistance [C/W]	Effective Gap [mm]
416 ground stainless (3-25atm)	0.0025	0.000264	0.0069
304 ground stainless (40-70atm)	0.0011	0.000528	0.0137
ground aluminum (12-25atm)	0.0025	0.000088	0.0023
ground aluminum (12-25atm)	0.00025	0.000018	0.0005
ground copper (12-200atm)	0.0013	0.000007	0.0002
milled copper (10-50atm)	0.0038	0.000018	0.0005

TABLE II
INTERFACIAL CONDUCTANCE AND INTERFACE GAP FROM MILLS [2]
(MODERATE PRESSURE AND USUAL FINISH)

	Interfacial Conductance [W/m^2/C]	Effective Interface Gap [mm]
Ceramic-Ceramic	500-3000	0.0087 – 0.0052
Ceramic-Metal	1500-8500	0.0031 – 0.0173
Graphite-Metal	3000-6000	0.0043 – 0.0087
Stainless-Stainless	1700-3700	0.0070 – 0.0153
Aluminum-Aluminum	2200-12000	0.0022 – 0.0012
Stainless-Aluminum	3000-4500	0.0058 – 0.0087
Iron-Aluminum	4000-40000	0.0006 – 0.0060
Copper-Copper	10000-25000	0.0010 – 0.0026

II. INTERFACE GAPS BETWEEN COMPONENTS

The accuracy of a motors thermal performance prediction is dependent upon the estimate of the many thermal contact resistances within the machine (e.g., stator lamination to housing, slot-liner to lamination, etc). A contact resistance is due to imperfections in the touching surfaces and is a complex function of material hardness, interface pressure, smoothness of the surfaces, and air pressure. The easiest way to implement thermal contact resistances in a design program is to base the thermal resistance on an average interference air gap. Books on general heat-transfer analysis such as Holman [1] and Mills [2] give typical values of thermal resistance [m^{2}C/W] and thermal conductance [W/m^2/C] to be expected between various materials for various root-mean-square (rms) surface roughness. The definition of rms surface roughness is the rms of the deviations of a surface from the reference plane [3]—typical values given by Janna [3] are 0.0001 mm for a mirror finish and 0.023 mm for a rough finish. The data given by Holman and Mills can be converted to equivalent air gaps by using a thermal conductivity for air of 0.026 W/m/C. The results are given in Tables I and II.

The effects of material hardness and surface roughness are clearly seen, the softer and smoother materials have the smallest effective gaps. For the typical material interfaces found in electrical machines, values of an interface gap for aluminum–aluminum are in the range 0.0005 to 0.0025 mm, stainless–stainless of 0.007 to 0.015 mm, aluminum–stainless of 0.006 to 0.009 mm and aluminum–iron of 0.0006 to 0.006 mm. These values can be used as first estimates of interface gaps in electrical machine analysis.

The problem in using interface gap data such as those given in Tables I and II is that they do not account for some complexities associated with electrical machines. For instance, the gap between lamination and housing is a function of how well the rough laminated outer surface of the stator is prepared before the housing is fitted. This interface is further complicated when features are stamped on the outer surface of the lamination to help the stacking operation. Also, if the housing is made from aluminum which is soft compared to a cast iron frame, a reduced effective gap should result. However, this reduction is often not realized at high temperatures as the difference in thermal expansion rates between the hosing and stator lamination give rise to an increasing effective gap with temperature—often eliminating the softness advantage. Complexities associated with the slot-liner to lamination interface are that the liner material is quite pliable, the slot surface is laminated, the gap may be filled or partially filled with impregnation, and that a large slot-fill will tend to push the liner toward the lamination.

A test program is well underway to help identify typical gaps in different sizes of machine and to relate the gaps to manufacturing and material differences between machines. Table III shows typical values of lamination to housing interference gap found in a range of machines. These have been measured by passing a known loss through the interface and measuring the temperature on each side. The average of the values in the table is 0.037 mm, but the gap can vary significantly depending upon the manufacturing process and materials used. The gaps found are typically around ten times greater than those found in Tables I and II.

The user can easily examine the importance of interface gaps in their machine by varying them between expected upper and lower limits. The designer will get more accurate results if they can perform calibration based on testing of motors that are constructed using materials and manufacturing processes to be used in their new designs.

III. WINDING MODELS

In electrical machines that have random wound mush winding, it is not possible or desirable to model the position of each individual conductor when carrying out thermal analysis. Even when using precision and form wound windings, it is not necessary to model each individual conductor to predict the temperature distribution accurately. In many cases, end windings are of a more random nature than the active section of the motor. In the past, various modeling strategies have been developed in the past to model the heat transfer and temperature distribution within a winding:

- composite thermal conductivity [4];
- direct equations bases on conductor geometries [5];
- T-Equivalent circuit for thermal resistance [6].

All of the above are suitable for inclusion in lumped circuit programs and each has its own advantages and disadvantages.

The composite thermal conductivity can be considered a simple solution but it requires the determination of the equivalent thermal conductivity $(k_{cu,ir})$ of the air and insulation material in the slots. This equivalent thermal conductivity depends on several factors, such as the materials, quality of the

Motor	Effective Interface Gap [mm]
4kW TEFC IM (M112M4 in Fig 1)	0.042
7.5kW TEFC IM (M132M4 in Fig 1)	0.076
15kW TEFC IM (M160L4 in Fig 1)	0.077
30kW TEFC IM (M200L4 in Fig 1)	0.016
55kW TEFC IM (M250M4 in Fig 1)	0.037
142mm cast aluminum housing BPM	0.01
range of 335mm − 500mm cast iron IM's	0.015
130mm diameter aluminum IM	0.02
Average of above data	0.037

Fig. 2.   Equivalent thermal conductivity in the stator slots.

Fig. 3.   Layered winding model suitable for electric machines.

impregnation, and residual air quantity after the impregnation process. If $k_{\mathrm{cu,ir}}$ is known, the thermal resistance between the winding and the stator lamination can be computed using the following equation:

$$R_{\mathrm{cu,ir}} = \frac{t_{\mathrm{eq}}}{k_{\mathrm{cu,ir}} A_{\mathrm{slot}}} \qquad (1)$$

where

t_{eq} equivalent thickness of the air and all the insulation material in the stator slots;

$k_{\mathrm{cu,ir}}$ equivalent conductivity coefficient of the air and insulation material in the stator slots, evaluated by dc supply experimental test;

A_{slot} interior slot area ($A_{\mathrm{slot}} = l_{\mathrm{sb}} L_{\mathrm{s}}$)

$$t_{\mathrm{eq}} = \frac{S_{\mathrm{slot}} - S_{\mathrm{cu}}}{l_{\mathrm{sp}}} \qquad (2)$$

S_{slot} stator slot surface;
S_{cu} copper surface in the stator slot;
l_{sp} stator slot perimeter.

From tests performed on the motors reported in Fig. 1 [4], the obtained values of the equivalent thermal conductivity are reported in Fig. 2 as a function of the stator filling factor. The linear regression reported in the picture can be written as

$$k_{\mathrm{cu,ir}} = 0.1076 * k_{\mathrm{f}} + 0.029\,967 \qquad (3)$$

where a value of $k_{\mathrm{cu,ir}}$ equal to the air thermal conductivity for a filling factor k_{f} equal to zero has been imposed. It is evident that the equivalent thermal conductivity increases with the stator slot filling factor. Taking into account that the filling factor used in industrial TEFC induction motor is in the range $0.35 \div 0.45$, the equivalent thermal conductivity can be considered in the range of 0.06 to 0.09.

A requirement of the winding model incorporated in the thermal simulation software was that it should be simple to understand and ease visualization of results. To achieve this, a new method was developed based on a layered winding model. A depiction of the model is shown in Fig. 3. In the model, we try to lump conductors together having similar temperatures. Layers of copper that have roughly equal temperature are expected to be a similar distance from the lamination. The layers start at the slot boundary with a lamination to slot liner interface gap (Section II; this can be an air/impregnation mixture), then
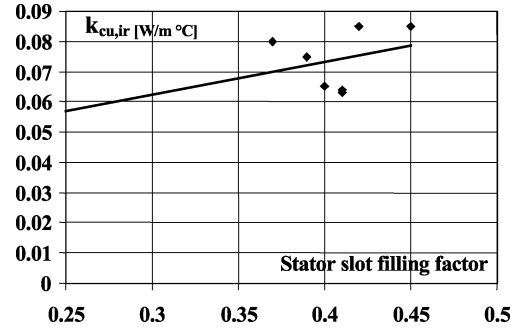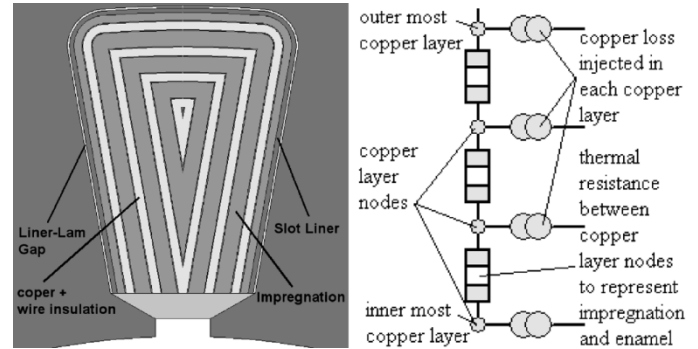
a slot liner (known thickness), and then layers of impregnation, wire insulation, and copper. A drawing of the layered model is shown in Fig. 3. This is to help the user visualize the slot fill and show where the hot spot is likely to be. It is also useful for spotting errors in data input. It is assumed that heat transfer is through the layers thickness. The series of thermal resistances is also shown in Fig. 3. It is easy to calculate the resistance values from the layer cross-sectional area, thickness, and material thermal conductivity. For a given slot fill, if small strands of wire are selected, then more conductors result. In such cases, you would expect more effective gaps between conductors and to have more copper layers. To achieve this, we make the copper layer thickness equal to that of the copper bare diameter. The winding algorithm then iterates with the spacing between copper layers until the copper area in the model is equal to that in the actual machine. This sets the number of copper layers. The slot area left after inserting the liner and copper layers is copper insulation and impregnation. A similar constraint is also placed on the wire insulation in that the model insulation area is equal to that in the real machine. The only other parameter that needs to be set in the model is how thick the first layer of impregnation is in comparison to the rest. The default values used in the program are half the thickness of the other layers. This is because typically many of the round conductors will be in contact with the liner surface.

The beauty about the model is that we can simply apply impregnation goodness factors to analyze the effect of air within the impregnation using a weighted sum of impregnation and air thermal conductivity. Typically larger impregnation goodness factors can be achieved with vacuum impregnation rather than trickle or dip varnish processes [7].

IV. CONVECTION FROM HOUSING SURFACE

Within the heat-transfer literature, there are many empirical correlations that are suitable for the prediction of convection cooling from surfaces shapes typically seen in electrical machines [1]–[3]. For instance, correlations exist for natural and forced convection from simple shapes, such as cylinders and flat plates, and more complex structures, such as open and closed channels of various shapes and sizes. Such correlations are usually based on the dimensionless numbers: Reynolds (Re), Grashof (Gr), Prandtl (Pr), and Nusselt (Nu) numbers. For natural convection, the typical form of the correlation is

$$\mathrm{Nu} = a(\mathrm{Gr}\,\mathrm{Pr})^b. \tag{4}$$

For forced convection, the typical form is

$$\mathrm{Nu} = a(\mathrm{Re})^b(\mathrm{Pr})^c \tag{5}$$

where a, b, and c are constants given in the correlation. Also

$$\mathrm{Re} = \frac{\rho v L}{\mu} \tag{6}$$

$$\mathrm{Gr} = \frac{\beta g \Delta \mathrm{T} \rho^2 L^3}{\mu^2} \tag{7}$$

$$\mathrm{Pr} = \frac{c_p \mu}{k} \tag{8}$$

$$\mathrm{Nu} = \frac{hL}{k} \tag{9}$$

where
h heat-transfer coefficient [W/m^2/C];
μ fluid dynamic viscosity (kg/s.m);
ρ fluid density (kg/m^3);
k fluid thermal conductivity (W/m/C);
c_p fluid specific heat capacity (kJ/kg/C);
v fluid velocity (m/s);
ΔT delta temperature of surface-fluid (C);
L characteristic length of the surface (m);
β fluid coefficient of cubical expansion $1/(273 + T_{\mathrm{FLUID}})$ (1/C);
g   gravitational force of attraction (m/s^2).

The magnitude of Re is used to judge if there is laminar or turbulent flow in a forced convection system. Similarly, the Gr.Pr product is used in natural convection systems. Turbulent flows give enhanced heat transfer but added resistance to flow in a forced convection system.

The parameter that we are ultimately after is h. Once we know h, we can calculate a thermal resistance to put in the lumped circuit model using the relationship

$$R = \frac{1}{Ah} \tag{10}$$

where
R thermal resistance (C/W);
A surface area (m^2);
h convection heat-transfer coefficient (W/m^2/C).

Natural convection heat transfer is a primary function of the temperature difference between component and fluid and the fluid properties. Forced convection is a primary function of the fluid velocity and fluid properties and only a secondary function of the temperature because fluid properties are temperature
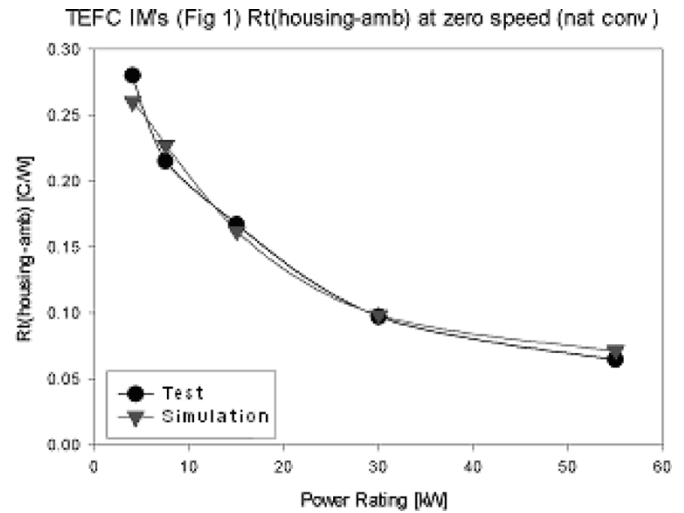

Fig. 4.   Natural convection resistance between frame and ambient air.

dependent. It is often easier to predict the heat transfer due to natural convection as we do not need to predict the local fluid velocity. This is usually true in machines intended for natural convection as they either have relatively smooth well-defined surfaces or include radial fins that are intended for natural flow in the inter-fin channels. For such cases, well-proven correlations exist.

Cases where the calculation is more complex are in TEFC machines where the use of axial fins does not lend themselves to inducing a good flow of natural convection air flow deep into fin channels. We must, however, be able to predict the natural heat transfer in such machines (as shown in Fig. 1) as motors with shaft-mounted fans are often operated close to the stall at which point natural convection dominates. Special formulations have been developed to give an accurate calculation in such situations. Area-based composite correlations are used for the complex finned shapes with each part of the geometry using a correlation that is best suited to its shape and orientation [i.e., a combination of vertical flat plate, horizontal flat plate (upper and lower facing), cylinder and horizontal fin channel correlations]. Also, terms are introduced to limit dissipation area to a depth down the fin channel equal to fin spacing as there will be little air circulation at the base of deep narrow axial channels fitted to the sides of the motor. A special form of average is used such that if the fins are deep compared to spacing, then the fin-side correlation predominates, but if the fins are not deep, then the fin base correlation predominates. This ensures that when the fins are virtually nonexistent, then the correlation reverts back to that of a cylinder or square tube. Fig. 4 shows that in TEFC that a good prediction of the natural convection can be achieved using such complex correlations. Here, we see both calculated and measured thermal resistance values between housing and ambient for the motors shown in Fig. 1; the fan being at rest in this case. The calculated data have been done adopting the default setting of all parameters—all the user has done is input the geometry for the motor and its foot mounting (the cooling from the flange or foot mounting is important and is included in the analysis), the winding details, the materials, and the losses.
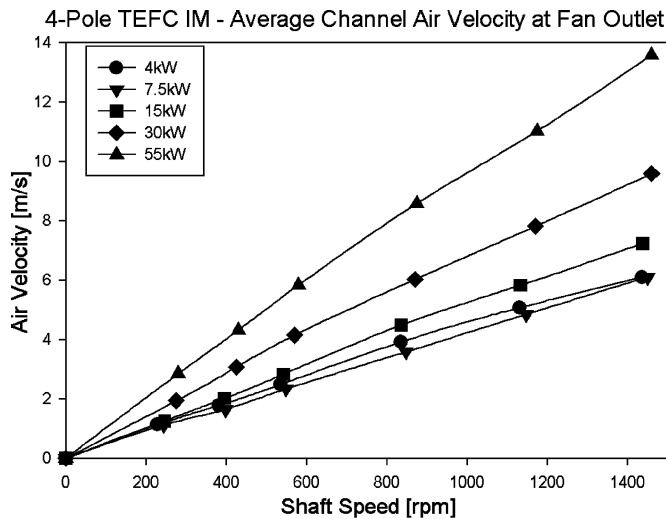
Fig. 5. Variation in fin channel air velocity (average at fan outlet) with rotational speed for the motors in Fig. 1.
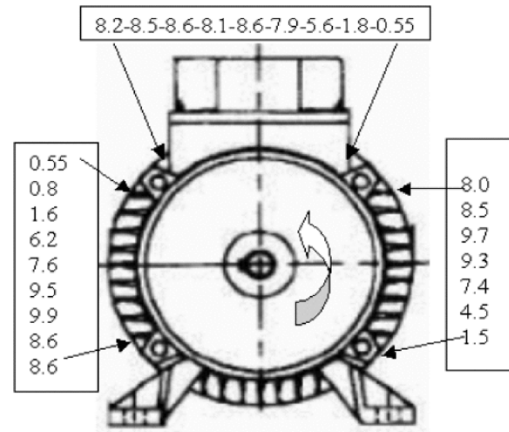

Fig. 6. Typical form of variation in fin channel air velocity with fin position (reported speed in meters per second).

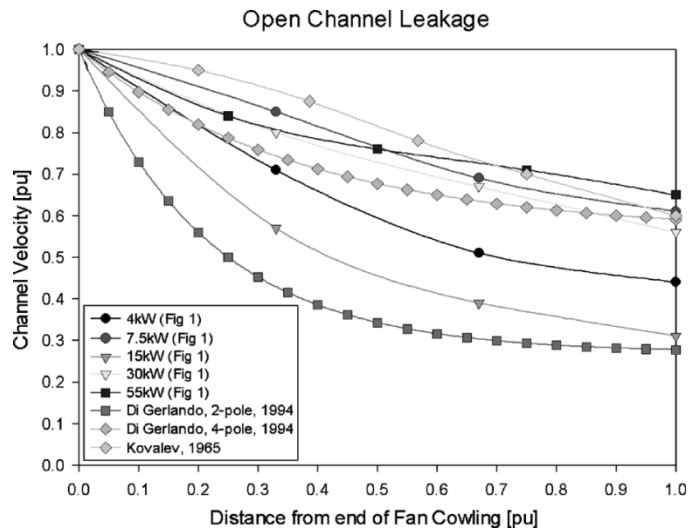Fig. 7. Typical form reduction in local fin channel air velocity with distance from the fan.

The mixed heat transfer due to the combination of natural and forced convection is estimated using the formulation [8]

$$h_{\mathrm{MIXED}}^3 = h_{\mathrm{FORCED}}^3 \pm h_{\mathrm{NATURAL}}^3 \qquad (11)$$

where the motor orientation determines the $\pm$ sign used, a $+$ sign for assisting and transverse flow, and a $-$ sign for opposing flows.

In some forced convection systems, such as liquid cooled machines, the fluid velocity is well defined (from the flow rate and the known ducting cross-section). However, in TEFC machines with open fin channels, the prediction of the local fluid velocity can be more difficult. It is important to include channel blockage and leakage factors to try and help the user determine accurate velocities. The correlation used for open fin channel constructions is that of Heiles [9]. This is based on testing actual electric motors. In the correlation, it is assumed that the flow is always turbulent due to the fact that the radial fans and cowlings used in such machines create turbulence.

The inlet velocity to the fin channels must be estimated. We can use empirical data such as that shown in Fig. 5. This shows that average velocity of the air in the fin channels as it leaves the fan. The variation in velocity with shaft speed is as expected, a linear relationship. The actual variation in velocity from channel to channel can vary significantly and is a function of the fan direction, as shown in Fig. 6. Alternatively, we may know the volume flow rate. As we know from the channel dimensions and the inside diameter of the cowling, we can calculate the velocity from the cross-sectional area available for flow.

A. Open Fin Channel Blockage and Leakage

Typically in a TEFC machine, some of the fin channels on the outside of the machine are blocked by bolt lugs and terminal boxes. Another deficiency of TEFC machines is that the air leaks out of the open channels causing the local air velocity to be lower at the drive end than at the nondrive end. The typical form of the reduction in velocity is shown in Fig. 7. The prediction of the actual reduction in velocity is a complex function of many factors including the fan, fin, and cowling design and rotational

speed. A more accurate model is formed if some calibration is performed using testing and/or CFD as shown in Figs. 5 and 7. Fig. 8 shows the typical accuracy that can be expected with an uncalibrated model. Here, we have taken software default parameters and calculated the effective thermal resistance between housing and ambient. The open channel air leakage data of Di Gerlando [10] in Fig. 7 is used as defaults in this case. It is seen that an accurate estimate can be made if the user has a basic knowledge of the inlet air velocity or volume flow rate to the fin channels. From Fig. 4, it is seen that the larger machines have a higher air speed, this being confirmed by comparing calculated and measured data in Fig. 8. Fin blockage is simply accounted for by the user counting the total number of fin channels (N_{total}) and the blocked channels N_{block}. The factor used is then

$$\frac{N_{\mathrm{total}} - N_{\mathrm{block}}}{N_{\mathrm{total}}}. \qquad (12)$$

Kovalev [11], [13] has performed testing on open and closed fin channel arrangements. He shows that the reduction in heat transfer is only of the order of 10% in the open-channel arrangement; the inlet velocity to both being the same. The small reduction compared with the larger reduction in velocity along the
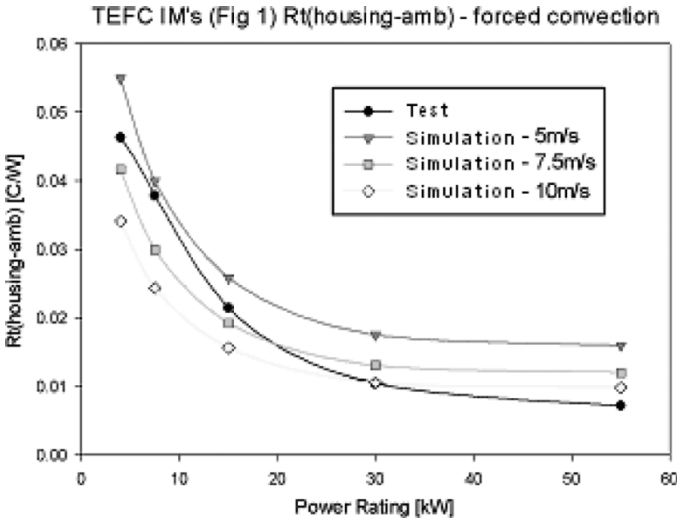
Fig. 8. Forced convection resistance between frame and ambient air.

Fig. 9. Published end space convection correlations.

channels is attributed to additional turbulence in the middle and far end of the machine. The closed fin channel requires a larger driving force in terms of a larger fan. Benerke [12], [13] shows similar results.

V. END SPACE COOLING

The end-space is defined as the area within the end-shields that contains the end winding, end cage (in induction machines), and any simple fans. This area of machine cooling is known to be one of the most difficult to predict accurately. This is because the fluid flow (air in most cases) in the end space region of an electric motor is usually much more complex than that for flow over its outer surfaces. The flow depends on many factors including the shape and length of the end winding, added fanning effects due to wafters and salient poles, the surface finish of the end sections of the rotor and turbulence. Not withstanding the complexity, several authors have studied the cooling of internal surfaces in the vicinity of the end winding [6], [10], [13], [14]–[17]. Some have based their results on testing and some on CFD. In the majority of cases, they propose the use of a formulation of the form

$$h = k_1(1 + k_2 \text{vel}^{k3}) \qquad (13)$$

where

h	heat-transfer coefficient (W/m^2/C);
k_1, k_2, k_3	curve fit coefficients;
vel	local fluid velocity (m/s).

The k_1 term accounts for natural convection and the $k1 \times k_2 \times$ vel^{k3} term accounts for the added forced convection due to rotation.

Fig. 9 compares published correlations for end-space cooling, where relatively good correspondence is shown for such a complex phenomena. The accuracy of CFD in predicting the local heat transfer is not guaranteed, but it is usually good at predicting local velocity variations [17]. This information can be usefully employed by analytical packages to give more accurate models.
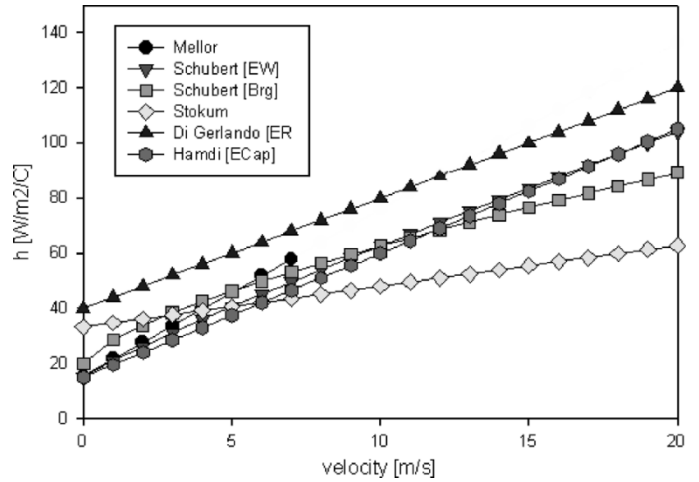
VI. AIR-GAP HEAT TRANSFER

The traditional method for accounting for heat transfer across air gaps in electrical machines is to use the dimensionless convection correlation developed from testing on concentric rotating cylinders first by Taylor [22] in 1935 and then added to by Gazley [23] in 1958. In the analysis, use is made of the Taylor (Ta) number to judge if the flow is laminar, vortex, or turbulent

$$Ta = \text{Re}\sqrt{\frac{l_g}{R_r}} \qquad (14)$$

$$\text{Re} = \frac{\rho l_g v}{\mu}. \qquad (15)$$

Equation (15) is useful for a system with the presence of a small air gap. The flow is laminar if $Ta < 41$. In this case, $\text{Nu} = 2$ and heat transfer is by conduction only. If $41 < Ta < 100$ the flow takes on a vortex form with enhanced heat transfer

$$\text{Nu} = 0.212 \, Ta^{0.63} \text{Pr}^{0.27}. \qquad (16)$$

If $Ta > 100$, the flow becomes a fully turbulent flow and a further increase in heat transfer results

$$\text{Nu} = 0.386 \, Ta^{0.5} \text{Pr}^{0.27} \qquad (17)$$

where

R_r	rotor radius (m);
l_g	air-gap length (m);
ρ	fluid density (kg/m^3);
μ	fluid dynamic viscosity (kg/s.m).

The problem with the above formulation is that the slot opening and, in extreme cases, salient poles are not included. Published data that include saliency are quite scarce. Gazley [23] does look at the slot opening and finds that if the flow is laminar, then there is a decrease in heat transfer compared to the smooth air gap. If the slots are on the rotor, then the reduction is by around 10%. If the slotting is on both surfaces, then this decrease can be as large as 20%. If the flow is turbulent, then there can be a significant increase in heat transfer. In the vortex flow range then there is little difference to that of the
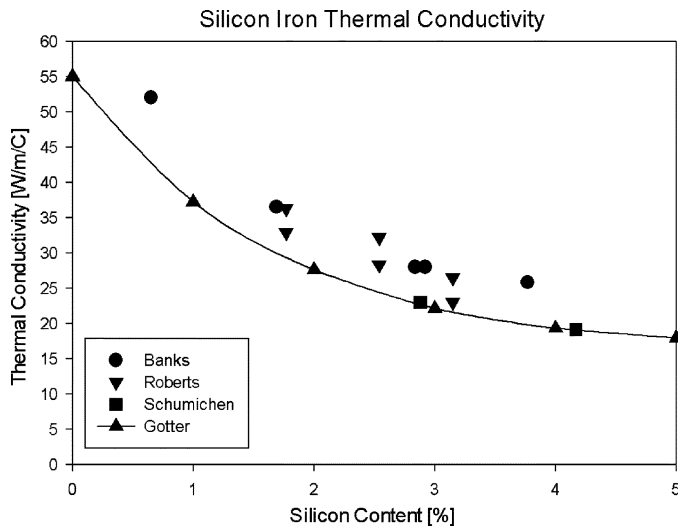
Fig. 10. Variation of thermal conductivity with lamination silicon content.

Fig. 11. Adopted system for the bearing temperature measurement.

smooth cylinder. Hazley [24] carries out computational fluid dynamics (CFD) on smooth air gaps and rotor and stator salient pole structures (larger cavity than slotting). He shows a 10% increase in heat transfer (taking the same air gap area as for the smooth air gap) for stator saliency and a 20% increase for rotor saliency. He does not give results for both rotor and stator saliency as found in switched reluctance machines.

VII. MATERIAL DATA

A thermal model is only as good as the material data put into it. There are a number of common deficiencies associated with data for materials used in electrical machines. One of the main deficiencies is the lack of thermal data provided by steel manufacturers—typically they do not publish thermal conductivity data for silicon iron. As can be seen from Fig. 10, the thermal conductivity is a function of the silicon content [13], [18]–[21]. Steel manufacturers also tend not to publish the chemical makeup of the steel.

The difference in lamination stack radial and axial lamination conductivities is an area that requires more research. The effective axial thermal conductivity is a complex function of such aspects as the clamping pressure, lamination thickness, stacking factor, lamination surface finish, and interlamination insulation material [13], [19], [25]. Typical ratios of radial-to-axial thermal conductivity are 20 to 40 [13], [25], [26].

Obtaining thermal conductivity data for critical materials such as the slot liner and impregnation can also be difficult. This situation is, however, improving with time as more motor manufacturers ask for such data from component suppliers. Also, there have been developments in improved insulation systems which have higher thermal conductivities. In such cases, their thermal properties are published as they are selling points for the materials.

VIII. BEARINGS AND END SHIELDS

The bearing thermal model is not a simple problem. The bearing is a complex mechanical component from the thermal point of view. In partic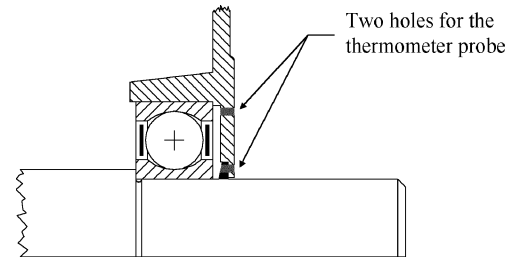ular, the balls are in contact with the inner and outer rings just in a very small mechanical spot and, as a consequence, the thermal transfer is difficult to predict accurately. In addition, inside the bearing, the presence of grease and lubricant introduces new factors of uncertainty for thermal resistance determination.

A simple solution is to consider the bearing as an equivalent interface gap. The authors are working on gathering more data on typical values for this equivalent gap. To date, some of the motors shown in Fig. 1 have been tested. The procedure adopted is as follows. A thermal model of the motor under test is calibrated using the temperatures measured during a dc supply test. The thermal model is considered calibrated when the predicted temperatures match the measured ones. In this test, the rotor is at zero speed and only stator joule losses are present. A thermal exchange between housing and ambient is by natural convention and radiation. The critical thermal resistances that are calibrated are those that have been previously discussed in this paper [i.e., housing-lamination interference gap, winding model, housing natural convention (Fig. 4), etc.]

The second step is to perform a classical locked rotor test using a three-phase sinusoidal supply. In this condition, the mechanical losses are again zero because the rotor speed is zero. The active losses are the stator and rotor ones only. The rotor losses can be computed as the difference between the input power minus the stator joule losses as given in the following equation:

$$P_{\mathrm{jr}} = P_{\mathrm{input}} - 3R_{\mathrm{s}}I_{\mathrm{s}}^2 \tag{18}$$

where

P_{jr} rotor Joule losses;
P_{input} input electrical power;
R_{s} stator resistance;
I_{s} stator current.

In order to measure the temperature of the inner and outer bearing rings during these tests, a special end shield has been adopted as shown in Fig. 11.

The dc calibrated thermal model has shown very good agreement between the measured and predicted temperatures for the windings, stator lamination, and housing during the locked rotor thermal simulation. Starting from this thermal model, the front and rear equivalent bearing interface gaps have been changed until the temperature across the bearing thermal resistance is equal to the measured one. The obtained equivalent bearing interface gaps are reported in Table IV for several bearings. The obtained results seem to be interesting even if the test has been made with the rotor and the bearing at stall. In particular, these first results show that a bearing equivalent interface gap equal

TABLE IV
BEARING EQUIVALENT INTERFACE GAP

Motor	Inner Diameter [mm]	Outer Diameter [mm]	Width [mm]	Equivalent interface gap [mm]
4 kW	30	72	19	0.35
7.5 kW	40	80	18	0.23
15 kW	45	100	25	0.40

to around 0.3 mm can be considered in a thermal model first approach. The authors are now working on suitable tests for defining the bearing thermal behavior with the rotor in running condition.

If the predicted bearing temperature contact resistance difference is to be predicted accurately, an accurate model of the motor end shields is also required. It is possible to predict both radial and axial thermal resistance values for the end shields if their effective lengths and cross-sectional areas are known. However, this is often complicated when the end shields have complex shapes. The interference fit to the housing must also be taken into account. The authors are working on this problem and the results will be presented in the future.

IX. CONCLUSION

In this paper, some of the more difficult aspects of electric motor thermal analysis have been discussed. It is evident that a superficial knowledge of the geometrical and material properties used in a machine's construction is not sufficient to give an accurate prediction of the thermal performance. This is because many of the complex thermal phenomena that occur in electric machines cannot be solved by pure mathematical means. Even powerful numerical programs based on computational fluid dynamics do not give any assistance in solving problems, such as the identification of interface gaps between components, the development of accurate winding and bearing models, etc. The interface gap between the housing and lamination stack is a function of the material softness and manufacturing processes used and the winding model is a complex function of slot-fill, the slot liner, the impregnation, the winding process, etc.

The CFD's main strength is in the visualization of fluid flow. An example of such visualization is in the prediction of the complex air flow in the end regions of electric motors. The use of CFD is expensive in computing terms, but such data can be used to improve the accuracy of analytical models. In most cases, empirical data are called upon to aid in the development of analytical models to solve thermal complexities. A classical case of the use of empirical data is in the development of convection correlations. More recent uses of empirical data are in setting realistic values for interface thermal resistance between components, the development of bearing models, calibration of winding models, and in the prediction of open fin channel air leakage.

In the design package, we have used both empirical data and CFD to set realistic values for the default parameters associated with the complexities talked about. Use of default values will get the user acceptable accuracy in most cases. However, experimental calibration based on materials and construction techniques used by the motor manufacturer can improve the accuracy further. For best reuse of calibration test data, it is best to set

up databases and/or define analytical curve-fitting equations to predict the key thermal quantities when designing new motors. This approach is welcomed by electrical machine manufactures to get the most benefit out of testing existing motors and prototypes and improve their future design capabilities. One good thing is that in uncalibrated CFD and analytical models, the user can gain great insight from trying out new design configurations and seeing by what percentage the temperatures increase or decrease—the absolute temperatures may be in error but the percentage change is usually realistic.

Analytical design packages have been found to be of great benefit in the identification of the key thermal design parameters. Based on analytical methods backed up by empirical and CFD data, they have very fast calculation speeds. This allows the user to perform instantaneous "what if" studies with variation in parameters between upper and lower expected limits. This sensitivity analysis is used to identify the key design variables that should be concentrated on if an optimum design is to be produced and to access what level may be varied before a substandard design results.

REFERENCES

[1] J. P. Holman, *Heat Transfer*. New York: McGraw-Hill, 1997.
[2] A. F. Mills, *Heat Transfer*. Englewood Cliffs, NJ: Prentice Hall, 1999.
[3] W. S. Janna, *Engineering Heat Transfer*. New York: Van Nostrand, 1988.
[4] A. Boglietti, A. Cavagnino, M. Lazzari, and M. Pastorelli, "A simplified thermal model for variable speed self cooled industrial induction motor," *IEEE Trans. Ind. Appl.*, vol. 39, no. 4, pp. 945–952, Jul./Aug. 2002.
[5] F. U. Braunschweig, *Die Warmeleitung in Runddrahtspulen*: Archiv Fur Elektrotechnik, 1995.
[6] P. H. Mellor, D. Roberts, and D. R. Turner, "Lumped parameter thermal model for electrical machines of TEFC design," *Proc. Inst. Elect. Eng., B*, vol. 138, no. 5, Sep. 1991.
[7] D. A. Staton, "Thermal computer aided design—advancing the revolution in compact motors," in *Proc. IEEE International Electric Machines Drives Conf.*, Boston, MA, Jun. 2001.
[8] F. P. Incropera and D. P. DeWitt, *Introduction to Heat Transfer*. New York: Wiley, 1990.
[9] F. Heiles, "Design and arrangement of cooling fins," *Elecktrotecknik und Maschinenbay*, vol. 69, no. 14, Jul. 1952.
[10] A. DiGerlando and I. Vistoili, "Thermal networks of induction motors for steady state and transient operation analysis," in *ICEM*, Paris, France, 1994.
[11] E. B. Kovalev, A. N. Burkovski, and A. T. Tokarenko, "Heat transfer in channels between frame-ribbing of enclosed asynchronous motors," *Elektrotechnika*, no. 11, 1965.
[12] W. Benecke, "Temperature field and heat flow in case of small surface cooled three-phase motors with squirrel cage rotor," *ETZ(A)*, vol. 87, no. 13, 1966.
[13] S. K. Pal, "Heat Transfer in Electrical Machines—A Critical Review," Rep., ERA Rep. 71-76, Jul. 1971.
[14] E. Schubert, "Heat transfer coefficients at end winding and bearing covers of enclosed asynchronous machines," *Elektrie*, vol. 22, Apr. 1968.
[15] G. Stokum, "Use of the results of the four-heat run method of induction motors for determining thermal resistance," *Elektrotechnika*, vol. 62, no. 6, 1969.
[16] E. S. Hamdi, *Design of Small Electrical Machines*. New York: Wiley, 1994.

[17] S. J. Pickering, D. Lampard, N. Hay, and T. F. Roylance, "Heat transfer from end-windings of a low voltage concentric-wound induction motor," in *Proc. Inst. Elect. Eng., Elect. Mach. Drives*, Durham, U.K., Sep. 1995.

[18] G. Gotter, *Heating and Cooling of Electrical Machines*. Berlin, Germany: Springer-Verlag, 1954.

[19] T. J. Roberts, "Determination of the thermal constants of heat flow equations of electrical machines," in *Proc. Inst. Mech. Eng.*, vol. 184, 1969–70, pp. 84–92.

[20] P. J. Banks, "Thermal Conductivity of Sheet Steel Laminations," Rep., AEI Manchester Rep. TP/R/1,188, 1961.

[21] M. Schumichen, "Longitudinal and transverse thermal conductivity of laminated transformer sheets" (in German), *Elektrie*, vol. 20, p. 12, 1966.

[22] G. I. Taylor, "Distribution of velocity and temperature between concentric cylinders," in *Proc Royal Soc.*, vol. 159, 1935, pp. 546–578.

[23] C. Gazley, "Heat transfer characteristics of rotating and axial flow between concentric cylinders," *Trans. ASME*, pp. 79–89, Jan. 1958.

[24] T. Hayase, J. A. C. Humphery, and R. Greif, "Numerical calculation of convective heat transfer between rotating coaxial cylinders with periodically embedded cavities," *Trans. ASME, J. Heat Transf.*, vol. 114, pp. 589–597, Aug. 1992.

[25] W. Liebe, "Cooling of large machines," *Elektrotech. Z (ETZ) A*, vol. 87, pp. 434–442, Jun. 1966.

[26] M. M. Liwschitz-Garik, "Some factors influencing the temperature rise of armature windings," *Trans. AIEE*, pt. III, vol. 74, 1955.
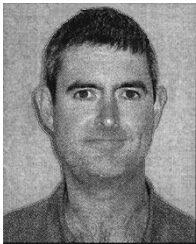
Dave Staton received the Ph.D. degree in computer-aided design (CAD) of electrical machines at Sheffield University, Sheffield, U.K., in 1980.

Currently, he is with Thorn EMI, the SPEED Laboratory at Glasgow University and Control Techniques, Glasgow, U.K., working on motor design and, in particular, the development of motor design software. In 1999 he set up a new company, Motor Design Ltd., Shropshire, U.K., to develop thermal analysis software for electrical machines.

Aldo Boglietti was born in Rome, Italy, in 1957. He received the Laurea degree in electrical engineering from the Politecnico di Torino, Torino, Italy, in 1981.

He began his research work as a Researcher in Electrical Machines with the Department of Electrical Engineering, Politecnico di Torino, in 1984. Currently, he is a Full Professor with Politecnico di Torino, where he was an Associate Professor in Electrical Machines in 1992. He is Head of the Electrical Engineering Department of the Politecnico di Torino until 2007. He is the author of many papers and his research interests include energetic problems in electrical machines and drives, high-efficiency industrial motors, magnetic material and their applications in electrical machines, electrical machines and drives models, and thermal problems in electrical machines.

Andrea Cavagnino was born in Asti, Italy, in 1970. He received the M.Sc. and Ph.D. degrees in Electrical Engineering from the Politecnico di Torino, Torino, Italy, in 1995 and 1999, respectively.

Currently, he is an Assistant Professor with the Electrical Machines Laboratory of the Department of Electric Engineering, Politecnico di Torino, where he has been since 1997. His fields of interest include electromagnetic (EM) design, thermal design, and energetic behaviors of electric machines. He has authored several papers published in technical journals and conference proceedings.

Dr. Cavagnino is a Registered Professional Engineer in Italy.